

# Segmented cells as tool for development of fuel cells and error prevention/prediagnostic in fuel cell stacks<sup>☆</sup>

M. Schulze<sup>\*</sup>, E. Gülzow, St. Schönbauer, T. Knöri, R. Reissner

*Deutsches Zentrum für Luft- und Raumfahrt e.V. (DLR), Institut für Technische Thermodynamik, Pfaffenwaldring 38-40, D-70569 Stuttgart, Germany*

Received 1 February 2007; received in revised form 16 March 2007; accepted 16 March 2007

Available online 30 March 2007

## Abstract

In the past various techniques to measure the current density distribution in PEFC were developed at the DLR Institute in Stuttgart. These techniques are used successfully to advance and to support the development of fuel cell stacks. Furthermore, the current density distribution measurements can also be used as a feedback control system to optimize the operation conditions, to avoid unfavourable conditions and to detect problems and defects at an early state. For this purpose three different techniques for determination of current densities were developed. In all techniques at least one of the flow fields is segmented. In an early design the individual segments are connected together with external resistances which are used for the measurement of the current density. This design is only suitable for the current density measurements in end plates of stacks or in single cells. Second, hall sensors are used to determine the current inside the segments. A recent development uses a design in which the segments as well as the resistances are realized in a printed circuit board (PCB) which can be used as a bipolar plate in stacks as well as in single cells.

Results can be used to validate models and to optimise components of a stack, e.g. flow field and manifold design, as well as the operating conditions of fuel cells. By applying segmented bipolar plates as sensor plates for system control integrated in stack systems high performance, safe operation and long life cycles can be achieved.

The main challenge in the development of control strategies based on current density measurements is their interpretation. Therefore, a simple and fast simulation of measured current density distribution has been developed taking into account the major influences on fuel cell performance (mainly the water management). As a result the actual local partial pressures, e.g. of oxygen and of water can be determined in short intervals and as a consequence a malfunction of the stack can be detected and avoided.

© 2007 Elsevier B.V. All rights reserved.

*Keywords:* PEFC; Current density distribution; Printed circuit board; Diagnostic methods

## 1. Introduction

For the development and the improvement of fuel cells and their operation a detailed understanding of the processes inside fuel cells and the local operation conditions is necessary. At the DLR various in situ and ex situ diagnostic methods are used in combination to study fuel cell behavior and fuel cell components. The low-temperature fuel cell activity of DLR focuses on polymer electrolyte membrane fuel cells and direct methanol fuel cells. The goals are in particular.

The understanding of complex behavior in cells based on the local operating conditions is necessary to optimize the fuel

cell components. For this purpose the local measurements in the cells are analyzed by simultaneous simulations. Furthermore, in order to increase the life time a detailed understanding of the degradations processes and their dependency on the operating conditions is necessary. Caused by the local variations of operating conditions and the local variation of the degradation processes it is useful to combine different analytic methods. The ex situ physical analytic methods are used to identify the degradation processes, the in situ electrochemical methods are used to quantify the effect of the performance decrease.

Another aspect is to support the development of fuel cell components and their manufacturing processes by analytical methods. The focus herewith is to identify problems associated with properties of specific components which are related to the local operation conditions. With this information a rational approach to improvements is possible. Examples are the development of flow fields and their interactions with

<sup>☆</sup> Based on the presentation at the in situ Diagnostics in Fuel Cell Systems Workshop, Düsseldorf, Germany, 29 June 2006.

<sup>\*</sup> Corresponding author. Tel.: +49 711 6862 456; fax: +49 711 6862 322.

E-mail address: [mathias.schulze@dlr.de](mailto:mathias.schulze@dlr.de) (M. Schulze).

the gas diffusion layers (GDL) as well as the development of electrodes. Another related topic is the development of strategies for quality control for fuel cell components.

Furthermore, information about the local reactivity can be used for the optimization of the operation of fuel cell systems. Different objectives can be fulfilled, namely the improvement of power density, cost reduction of fuel cell operation, the extension of life-time or improves reliability. An important application of in situ diagnostic tools is the control of the fuel cell system with the aim of minimizing malfunctions.

At the DLR various analytic methods and analytic equipment are used. For the ex situ analysis of fuel cell components – before and after fuel cell operation – the porosimetry measurements by mercury penetration and nitrogen adsorption, temperature programmed reduction (TPR), – oxidation (TPO) and desorption (TPD), X-ray diffraction (XRD), scanning electron microscopy (SEM) with energy dispersive X-ray spectroscopy (EDX), X-ray photoelectron spectroscopy (XPS) and thermogravimetry analysis (TGA, DGA) are used. In addition, presently a test facility for the investigation of time-resolved water sorption of membrane materials in combination with electrochemical impedance spectroscopy is being set-up.

For the analysis of operating fuel cells in situ methods are used, with are integrated in our test facilities. At the DLR approx. 20 test facilities for low temperature fuel cells, PEFC and DMFC [1], are used for the investigation of single cells, short stacks and stacks. Ten test facilities for SOFC characterization are operated for the characterization of single cells and stacks up to a power of 10 kW. All test facilities are controlled by a PLC system, which allows an automatic operation. The following measurements can be performed in the test rig:

- $V$ – $I$  characteristics,
- chronopotentiometry and chronoamperometry,
- electrochemical impedance spectroscopy (EIS),
- current density distribution (different versions, including temperature measurements),
- cyclic voltammetry (CV),
- analysis of the gas composition by gas chromatography.

The  $V$ – $I$  characteristics are routinely used to assess the electrochemical performance of the fuel cells whereas the chronopotentiometry and chronoamperometry allow to investigate the fuel cell behavior during changes of the operating conditions as well as to investigate the loss of electrochemical performance due to degradation processes. The electrochemical impedance spectroscopy is used to obtain a more detailed understanding of the processes inside the fuel cell. The EIS data allow to correlate the losses and components, namely the loss contribution of the anode, of the cathode or of the membrane. In addition, EIS helps to distinguish between transport processes and reaction processes [2]. Consequently, the electrochemical impedance spectroscopy is used for different investigations in the fuel cell. So it is necessary for a systematic optimization of the operating conditions. Furthermore, EIS in combination with ex situ methods is extremely helpful in the investigation of degradation processes, because the effect of the different degradation

processes on the electrochemical performance can be quantified individually.

Therefore, for most applications the combination of various in situ and ex situ methods is ideal. However, the locally resolved in situ measurement is an especially powerful tool for fuel cell research and development. Consequently, different methods for current density measurements have been developed. This paper is focused on the various current density measurement tools developed at DLR.

## 2. Experimental approaches and equipment for current density measurements

The variety of approaches to measure current density distribution in PEFCs that has been reported in the literature in the past years is huge. At Los Alamos National Laboratory the segmented cell approach, used before in electrolytic cells, was adapted to measure the current density distribution in fuel cells. The current collector plate of one of the electrodes contains 18 electrically isolated segments and the catalyst layer as well as the GDL were all segmented and electrically insulated [3]. A similar assembly was used in Ref. [4] to map the current distribution along a single flow channel. A segmentation of the membrane electrode assembly (MEA) was not necessary here.

Stumper et al. [5] described three different methods for the determination of the current density distribution. The first one, the partial MEA approach, operates with partially catalyzed MEAs or masked areas. It is suitable to analyze the performance of different regions of the cell. The second one involves electrical isolated subcells in both electrodes, the GDL and the flow field plates. Information about the current density at special locations in the fuel cell can be provided. In the third technique an array of resistors is placed between the non-segmented flow field plate and a buss plate. This current distribution mapping technique does not require any modification to the MEA or the flow field plates.

A modified subcell approach consists of isolated cylinders in a copper plate where the flowfield is milled-in [6]. Other groups designed flow field plates with single current collectors of gold plated stainless steel [7–10] or graphite plates [11] embedded in an insulating matrix.

The separation of the current generated at the electrode layer into electrically isolated paths is the common idea of all approaches. The current measurement of each path is done with an array of passive resistors or with separate load units. In some of the approaches the segmentation is extended to the GDL to prevent lateral currents due to in-plane conductivity. But any modification of these layers may entail a change in the properties of the assembly and complicates the use of the measurement systems. The described current distribution measurement methods have been developed for special investigations in laboratory single cells. Due to this fact they are not suitable for integration into fuel cell stack.

Another method is the measurement of the magnetic flux surrounding a fuel cell caused by the current inside the cell. With the so-called “Magnetotomography” the current distribution could

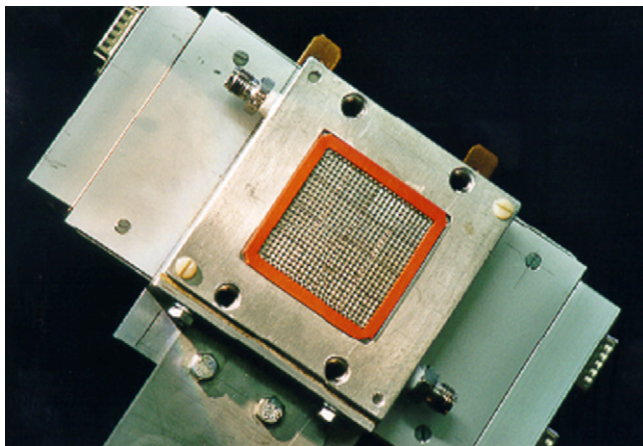


Fig. 1. Photograph of the laboratory segmented cell with 16 segments on an active area of  $5\text{ cm} \times 5\text{ cm}$  (scheme shown in Fig. 2).

be measured non-invasively even in stacks, but only qualitative results from single cells have been reported so far [12].

At DLR several diagnostic methods for locally resolved current density measurements in single cells and stacks were developed and used in PEFC, DMFC and SOFC. A short description of the different tools is given below.

One technique is based on individual segments which are externally connected with resistances for the current measurements in each segment. A photograph and a schematic diagram of this approach are shown in Figs. 1 and 2, respectively. The cell shown in Fig. 1 has an active area of  $5\text{ cm} \times 5\text{ cm}$  and 16 segments. All segments are isolated with PTFE among each other and the frame. Each segment is connected by a resistance to the current collector.

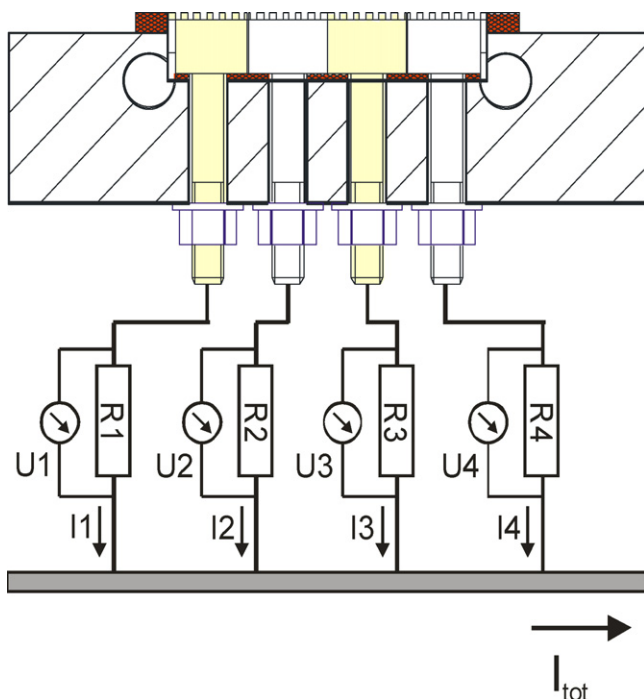


Fig. 2. Scheme of the laboratory cell for current density measurements with 16 segments, which allows more than  $2000\text{ samples s}^{-1}$ .

All segments must be positioned individually, which can cause some problems. In order to fit the surface of all segments in the same plane on the backside of the segments an elastic plate is used. If the elastic plate is too soft it is not possible to apply a high contact pressure from the flow field onto the GDL, which can result in high electrical contact resistance. As a result, the variation of the contact resistances for the individual segments with the GDL can be high. If the elastic plate is too hard, the segments will not be assembled in the same plane, and consequently the contact pressures and contact resistance for the individual segments with the GDL can vary as well. Therefore, it is necessary to choose the elastic material according to the specific membrane-electrode assembly and GDL. In addition, the segments have to be manufactured very precisely in order to minimize the in-plane positioning problem. Therefore, this approach to local measurements is time intensive and cost-intensive.

An additional problem of the individual positioning of the segments is that a complex flow field increases the experimental problems. Therefore, at DLR a chocolate wafer structure with perpendicular channels with 1 mm depth and 1 mm width is used. Typically the segmented side is used as anode because in a hydrogen supplied fuel cell the effect of the transport processes on the anode side has a lower influence on the cell performance compared to the cathode. In the DMFC the segmented side is mostly located at the anode in order to investigate the cathode processes. Alternately, a segmented cathode side is used with pure oxygen in order to investigate the anode flow fields. Caused by the external connection of the segments and the thickness of this measurement device, the technique is only suitable for single cells or at outer cells in short stacks. That these segmented cells can be used in the DMFCs is the main advantage of this technique [13,14]. The external connection of the segments to the current collector is also used in the segmented cell which was built up to investigate solid oxide fuel cells (SOFC) at  $800\text{ }^{\circ}\text{C}$ . This SOFC cell is described in detail in Ref. [15].

In the late 1990s a segmented cell technique using a non-contact magnetic loop array for sensing local currents was developed and built up at DLR [16–18]. In Fig. 3 scheme and the function of this method is shown. The current through the segments induces a magnetic field. The magnetic fields induced by the current in each segment are measured with hall sensors

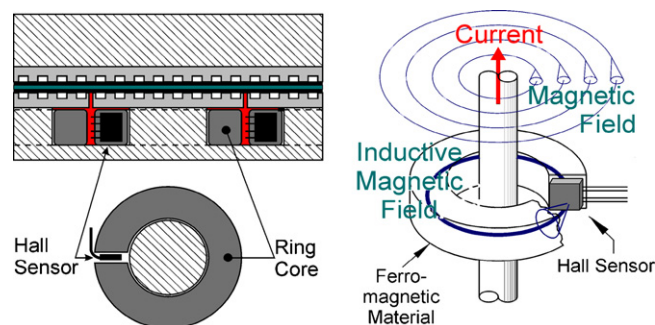


Fig. 3. Scheme of a segmented cell with hall sensors for current density measurement (left side) and function principle of the technique (right side) [16].

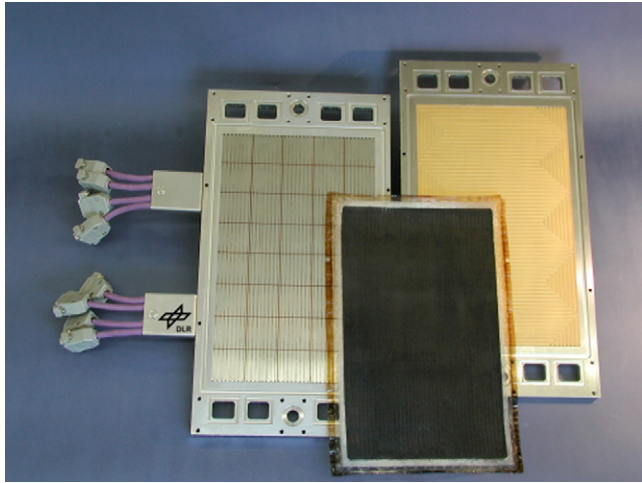


Fig. 4. Photograph of the segmented cell the hall sensor technique, which has 40 segments on an active area of  $600\text{ cm}^2$ , left side: segmented bipolar plate; middle used membrane-electrode assembly prepared with the DLR dry spraying technique and on the right side: the unsegmented plate [16].

positioned in slits of ferrite material rings which are surrounded the individual segments. This technique is described in detail in Refs. [16–18]. The low electric resistance of the plate as a result of the missing resistor array made this approach favourable for integration in a fuel cell stack. Therefore, the Hall sensor technique was used to design and to build up a bipolar plate with an active area of  $600\text{ cm}^2$  with 40 segments, which is shown in Fig. 4. Because of the temperature dependence of the resistance of the hall sensor this method can be used also for temperature measurements. However, the bipolar plate for the current density measurement has a thickness of approx. 1 cm, which is much thicker than a normal bipolar plate with one to a few millimeters. Consequently, the thermal behavior of the measurement tool is different from it of a normal bipolar plate.

Also in this technique the segments are mounted individually in the bipolar plate. The individual segments must be isolated from each other. In the case of the Hall sensor technique in-house the individual segments were isolated by silicone. In order to create an even surface plane for all segments, the active surface and the flow field is machined after mounting of the individual segments. Like for the technique with the external resistors the mechanical work and the time for setting up a bipolar plate with Hall sensor technique is also high. In addition the Hall sensors must be calibrated individually. These results in high costs for current density equipment based on Hall sensors. Therefore, this technique is also only for laboratory investigations but not for control systems. The Hall sensors can also be influenced by external magnetic fields especially by the current in the end plates; so the signals of the Hall sensors can be significantly disturbed if this technique is used in single cells or near the end plate.

The last development at DLR was the result of a search for a new current density distribution measurement tool with increased spatial resolution and reduced thickness for measurements in fuel cell stacks. The aim was to investigate regular cell operation without disturbances and errors. Therefore a segmen-

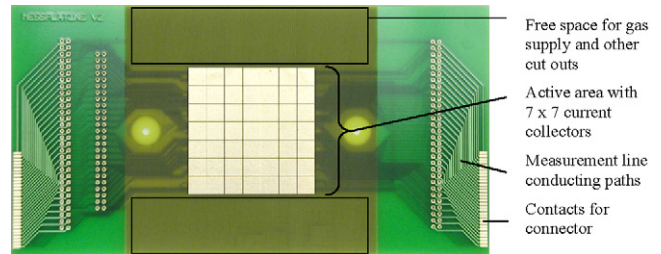


Fig. 5. Example of segmented bipolar plate with 49 segments for single cell and stack use (no flow field channels integrated).

ted bipolar plate with integrated current sensors was developed [19].

To realize a high integration package a printed circuit board (PCB) technology was chosen. This allows a flexible design of the shape and size of the current collector segments, which are placed on the surface of an epoxy-glass resin matrix (Fig. 5). The resistor array for the current measurement is integrated in the PCB using a multi-layer assembly. The flow field channels can be machined directly into the plate. The backside of the measuring plate is connected with an additional plate. In single cell use this is the gas supply and bracing plate. For stack application it can be either the endplate or the half of the bipolar plate containing the flow field structure of the next cell in the stack. In this interface cooling channels can be placed if necessary. The current collector segments of the measuring board are gold plated to decrease the contact resistance and to avoid corrosion. A detailed description of the assembly can be found in Ref. [20]. The measurement principle is shown in Fig. 6. The sense wire connectors on the segmented bipolar plate are connected to a data acquisition unit consisting of a multiplexer and a digital multimeter. The measurement set-up works independently from the electric load unit and the control system of the fuel cell.

The technique is realized with standard printed circuit board technology. The thickness of the used PCB was approximately 1.7 mm, but other thicknesses can be realized. A variety of measuring plates for different applications was produced and used in the last years. For laboratory use plates with 49 segments on an active area of  $25\text{ cm}^2$  were made and tested in single cells (Fig. 7). The tests showed that the measurement tool works very reliable and accurate. The single cell was operated under various conditions and the different current distributions could be analyzed. Segmented bipolar plates with  $6\text{ cm}^2$  active area and circular

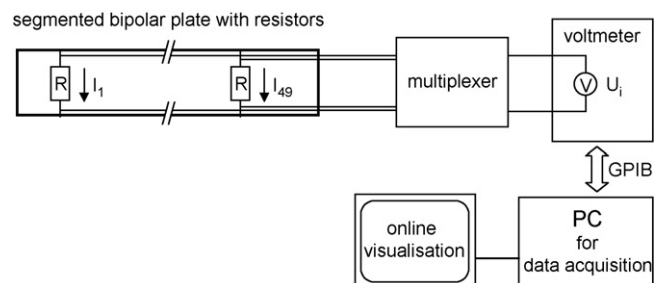


Fig. 6. Measuring system used for the segmented bipolar plate. Only the resistors for segment 1 and 49 are shown for clarity. A similar set-up is used for the laboratory cell shown in Fig. 1.

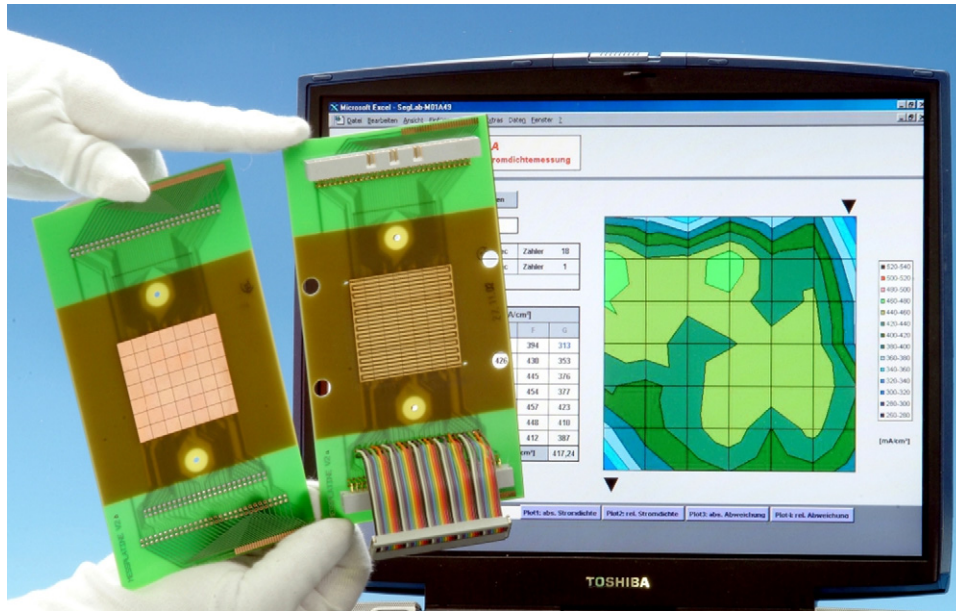


Fig. 7. Photography of the measuring plate (left) and a ready-made segmented bipolar plate with flowfield channels and measuring connectors next. On the display a measured current density distribution of a single cell with 49 segments on  $25 \text{ cm}^2$  active area is shown (right).

shape for microfuel cells were developed as well as plates with up to 108 segments for fuel cells in technical size of more than  $200 \text{ cm}^2$  active area.

Using segmented bipolar plates with a spatial resolution of  $0.5 \text{ cm}^2$  per segment a short stack consisting of three cells with an active area of  $25 \text{ cm}^2$  was assembled. All three cells were equipped with segmented bipolar plates for measuring the current density distribution in each cell. The current density distribution in the short stack with respect to the cell interactions could be studied [21].

For the current density measurements in PEFC the gas diffusion layer and the reaction layer are not segmented. Because of the moderate electric conductivity of the gas diffusion layer the interference between neighboring segments is relatively low; then for the current perpendicular to the segment cross the GDL the area is given by the segment area while the area for the current between neighboring segments is given by the length of the segment boundary and the thickness of the GDL. The length for the current transport is in the same range for both currents because the distance between the boundaries of two segments is in the same range as the GDL thickness. Consequently interferences between the segments do not adulterate significantly the current density measurements. The strength of the interference in the current density measurement depends on the anisotropy of the conductivity in the GDL and on the total conductivity of the GDL. As an example for a MEA with E-Tek ELAT single sided V3 gas diffusion layers an interference between neighboring segments approximately 10% of the difference in the current density was measured.

The current density distribution measurements are used for the optimization of the fuel cell components, especially the flow fields and electrode–electrolyte–electrode structures as well as for the optimization of operation conditions. In addition, the current density distribution measurements have a high potential for

use for the control of fuel cell systems and for the early detection of errors and failures in fuel cell stacks [22]. The current density measurements in combination with a simple simulation, which uses the current density as input data, allow to obtain information about the local operation conditions [23]. The combined use of locally resolved EIS and current density distribution measurements promises to yield novel information about fuel cell processes, which is of high interest for fundamental research to understand the fuel cell operation in detail but also for the improvement of components and operating conditions. Therefore, the tools for the current density measurements are adapted for locally resolved EIS measurements.

### 3. Examples for the use of current density measurements

In the following some examples of analytical studies of fuel cells at DLR are presented in order to show the potential of current density measurement in the fuel cell research, development and controlling.

#### 3.1. Improvement of DMFC by adaptation of the hydrophobicity of the GDL based on the data of current density measurements

As first example an improvement of the DMFC based on the data of the current density measurements will be presented. This work is reported in detailed in Ref. [24]. The base idea is not to use of the global  $V-I$  characteristics to determine the electrochemical performance of fuel cells and their components, which will be done routinely, but to use the locally resolved current density measurements. The measurements are performed in a single cell with the technique which uses the external interconnection of the segments. The active area was  $25 \text{ cm}^2$ . The cathodic gas inlet is

on top left, the used flow field in a serpentine flow field where the channel go up and down from left to right. The gas outlet is on bottom on the right side. The cell tests were performed at a cell voltage of 300 mV in the DMFC using different GDL on the cathode side. The operation conditions are 2.5 bar on the anode and 3.0 bar for the air. For the flow of the anode was set to  $10 \text{ mol min}^{-1}$  of a 1.5 mol  $\text{CH}_3\text{OH}/\text{H}_2\text{O}$ . The air flow was set to  $600 \text{ sccm min}^{-1}$  without humidification of the air. The direction of methanol–water–mixture flow on the anode was reverse to the cathodic gas flow.

First the current density distribution at 300 mV and the  $V-I$  characteristics were measured for a MEA with a low hydrophobic GDL and a strong hydrophobic GDL for anode and cathode. The current densities measured for the MEA with the low hydrophobic GDL (Fig. 8a) and for the MEA with strong hydrophobic GDL (Fig. 8d) differ significantly. For the MEA with the low hydrophobic GDL the current maximum is near the inlet. When the strong hydrophobic GDL is used the current maximum is shifted to gas outlet on the cathode. Using the GDL with the low hydrophobicity the water content in the cathodic gas is increases

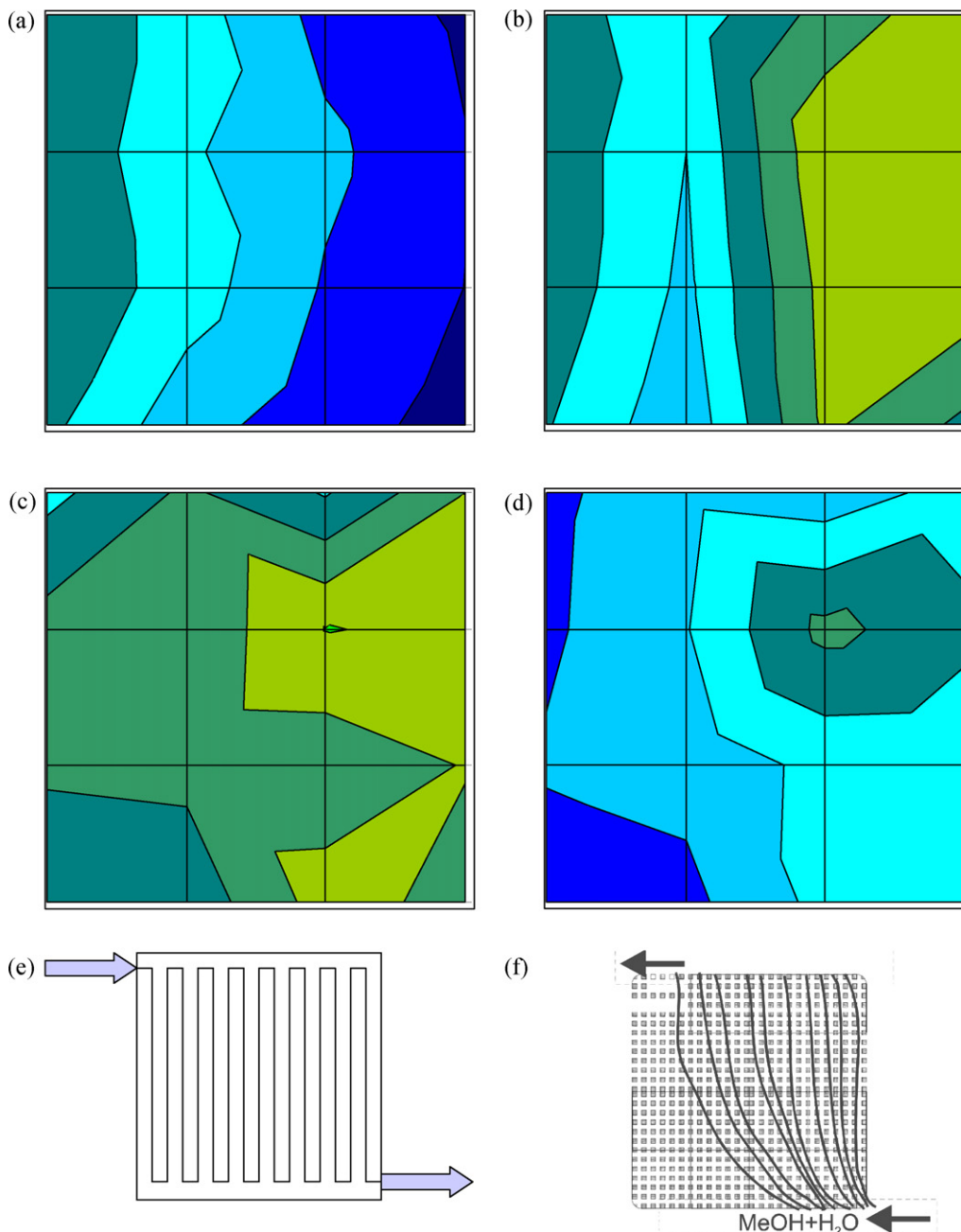


Fig. 8. Current density measured at cell voltage of 300 mV in the DMFC using different GDL. The operation conditions are 2.5 bar on the anode and 3.0 bar for the air. For the flow of the anode was set to  $10 \text{ mol min}^{-1}$  of a 1.5 mol  $\text{CH}_3\text{OH}/\text{H}_2\text{O}$ . The operation temperature was set to  $110^\circ\text{C}$ , (a) backing with a low hydrophobicity, (b) backing with a low hydrophobicity for the first half of the cell and a backing with a high hydrophobicity for the residual area, (c) backing with a low hydrophobicity for the first quarter of the cell and a backing with a high hydrophobicity for the residual area, (d) backing with a low hydrophobicity as shown in Fig. 9 below. The cathode flow is shown in (e) and the methanol flow on the anode is shown in (f).

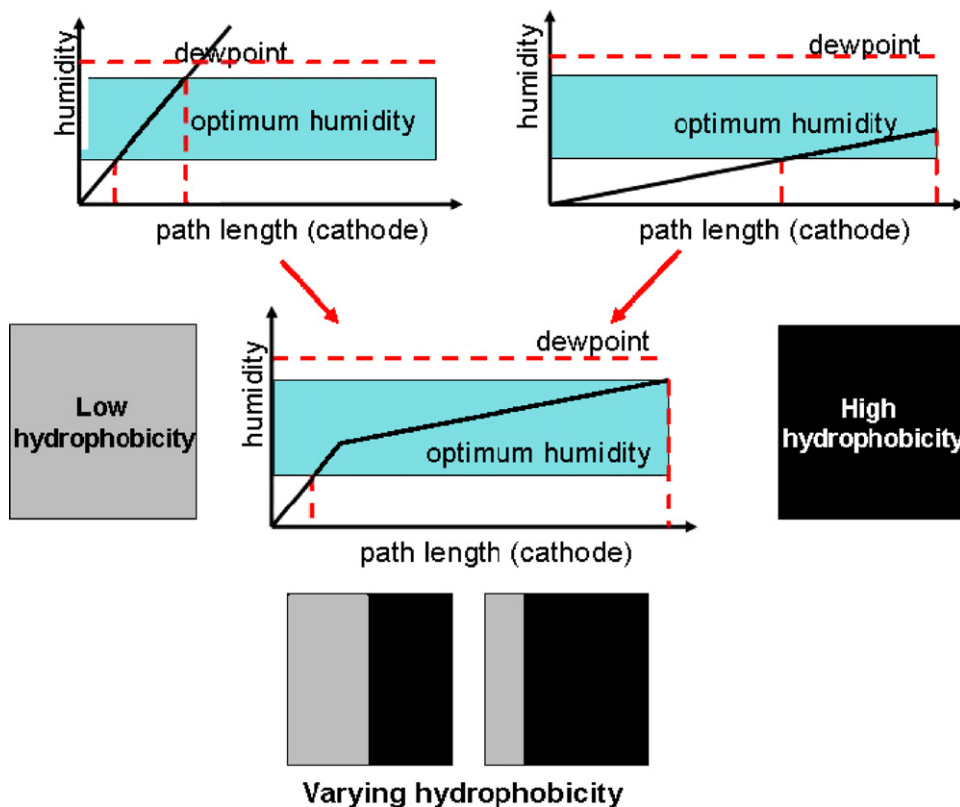


Fig. 9. Strategy for optimization of the hydrophobicity of the GDL in the DMFC.

along the gas channel rapidly with allows a good humidified membrane. This leads to high proton conductivity of the membrane, but also the high water content in the channel hinders the gas transport. Consequently the current maximum is located in the inlet range of the air flow.

In contrast for the strong hydrophobic GDL, the water content of the cathode along the channel is diminished and therefore, in the inlet range of the cathode the membrane is not well humidified. As a result a low proton conductivity of the membrane leads to a low electrochemical performance in this range. Along the channel the water content increases and the related proton conductivity increases and as consequence the current maximum is shifted along the channel in the direction of the outlet region.

Using this simple model, the idea shown in Fig. 9 was to grade the hydrophobicity of the GDL. This was realized by using the both GDL with different hydrophobicity for the preparation of the MEA (MEA). A scheme of the newly designed GDL is shown in Fig. 10. The corresponding current densities at 300 mA of two MEA with variation of hydrophobicity over the active area are



Fig. 10. Variation of the backings for the four different MEAs, which results are shown in Figs. 9 and 10. The gray areas are marked the GDL with a low hydrophobicity, the black area the GDL with the strong hydrophobicity. The cathodic gas inlet is on top left, the used flow field in a serpentine flow field where the channel go up and down from left to right. The gas outlet is on bottom on the right side.

shown in Fig. 8b and c. The current density distribution for both MEA becomes more homogeneous especially for the backing with a low hydrophobicity for the first quarter of the area and the backing with a high hydrophobicity for the residual area (Fig. 10c). This behavior indicates an improvement of the water management if a graded hydrophobicity in the GDL is used.

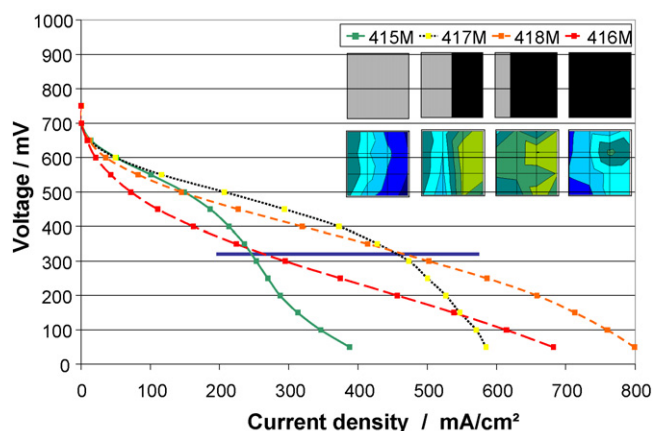


Fig. 11.  $V-I$  characteristics measured in the DMFC using different GDL. The operation conditions are 2.5 bar on the anode and 3.0 bar for the air. For the flow of the anode was set to  $10 \text{ mol min}^{-1}$  of a  $1.5 \text{ mol CH}_3\text{OH}/\text{H}_2\text{O}$ . The air flow was set to  $600 \text{ sccm min}^{-1}$  without humidification of the air. The operation temperature was set to  $110^\circ\text{C}$ , (a) backing with a low hydrophobicity, (b) backing with a low hydrophobicity for the first half of the cell and a backing with a high hydrophobicity for the residual area, (c) backing with a low hydrophobicity for the first quarter of the cell and a backing with a high hydrophobicity for the residual area, (d) backing with a low hydrophobicity as shown in Fig. 9 below.

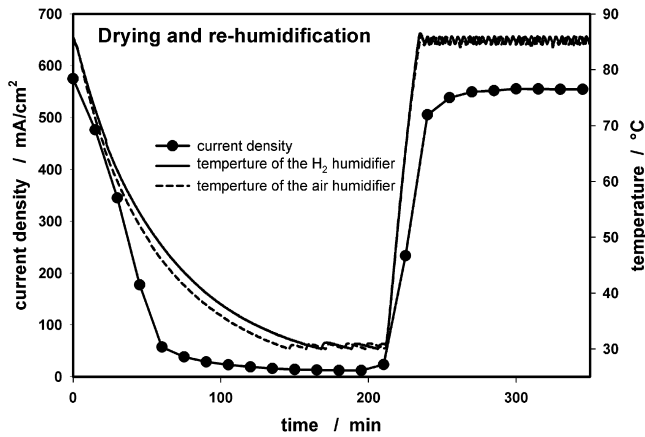


Fig. 12. Time dependence of cell current at 500 mV and temperature of the humidifier during reduction of the humidification and restart of the humidifiers.

For the benchmarking different MEA the current density distribution measured at 300 mV is not the crucial parameter but the  $V-I$  characteristics of the MEA. The  $V-I$  characteristics of the different MEAs are shown in Fig. 11. The MEA using the low hydrophobic GDL has a good performance at low current densities because only a low currents the water balance in the cell is equilibrated whereas at higher current densities the large

amount of water on the cathode hinder the gas transport and the performance is low. For the MEA with the strong hydrophobic GDL the electrochemical performance at low current densities as well as at high current densities is relatively low, but the  $V-I$  characteristic does not show a breakdown of the performance at high current densities with is typically for a transport limitation. With the graded GDL a good electrochemical performance at low current density like the MEA with the low hydrophobic GDL is archived and, in addition, the breakdown related tot the transport limitations is shifted significantly to higher current densities. Using the graded GDL the electrochemical performance is significantly improved; the combination of different GDL over the cell area in each electrode achieves a MEA with a wide range of excellent performance. As shown the data from the current density measurements are extremely helpful for the optimization of the fuel cell components like the GDL.

### 3.2. Investigation of drying and re-humidification in a single cell

The influence of the humidification of the fuel cell behavior was investigated by current density distribution measurements and electrochemical impedance spectroscopy [25]. In order to simulate an error – the breakdown of the humidification –

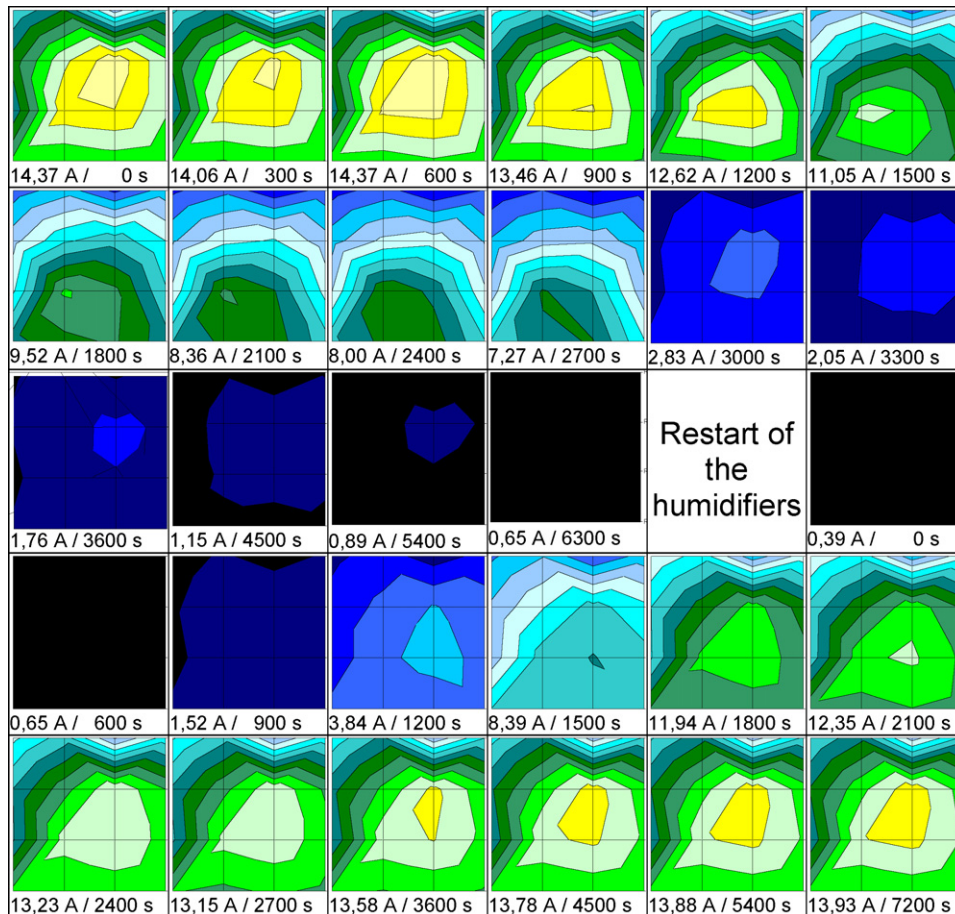


Fig. 13. Alteration of the current density distribution measured during drying the membrane and after restart the humidifiers at potentiostatically loading of 500 mV cell voltage at  $p_{H_2} = p_{air} = 2000$  mbar, flow rate  $H_2 = 6$  cm<sup>3</sup> s<sup>-1</sup>, flow rate air = 33.3 cm<sup>3</sup> s<sup>-1</sup>,  $\varphi_{air,max} = 66\%$ ,  $\varphi_{H_2,max} = 68\%$ , cell temperature = 75 °C.



the heaters of the bubblers which are used as humidifier was switch off. The cell was controlled potentiostatically at 500 mV, a cell temperature of 75 °C,  $p_{\text{H}_2} = p_{\text{air}} = 2000$  mbar,  $\text{H}_2$  flow rate =  $6 \text{ cm}^3 \text{ s}^{-1}$ , air flow rate =  $33.3 \text{ cm}^3 \text{ s}^{-1}$ . Fig. 3 shows the total current of the cell as well as the temperature of the humidifiers. The drop of their temperature down to room temperature results in a decreased humidification. If stable conditions were achieved, the humidifiers would have been restarted. The temperatures of the humidifiers and the resulting integral current density are given in Fig. 12.

As expected, after shut down of the humidifiers the cell performance decreases; the corresponding current density distribution is displayed in Fig. 13. During the drying process of the membrane the maximum in the current density distribution shifts from the middle of the cell to the outlet of the cell, because it takes longer for the outlet area to dry out. The water content increases along the flow field. As result, the local humidification is higher at the outlet and no liquid water is formed, which may block the pore system.

The expectation was that an inverse behavior compared to the drying experiment would be observed. But in contrast, the maximum of the current density does not shift significantly. After the restart of heating of the humidifiers the water content and the correlated ion conductivity of the membrane increases, because at the beginning the water take off into the membrane reduces the water content in the feed gas. After starting the humidifiers the local water content in the membrane is different in comparison to the end of the drying experiment. The water from the humidifier sorbs in the membrane, which reduce the humidification of the gas. Therefore the degree of humidification of the membrane and related proton conductivity of the membrane increases firstly in the inlet zone and consequently the maximum of current density distribution after re-starting the humidifiers is shifted to the gas inlets compared to it at the drying experiment.

The current density distribution measurement during drying and re-humidification of the MEA are different. Therefore, a problem with humidification can be derived from the current density distribution measurement, which indicates that the information of current density distributions can be used for controlling fuel cells.

#### 4. Conclusions

Different techniques for current density distribution measurements are used at the DLR for improvement of fuel cell components and for understanding fuel cell processes under normal operation as well as for the investigation of the effect of malfunctions on the fuel cell behavior.

For the single cell experiments the technique with the external resistance as well as the PCB technology are used, whereby the PCB technology is favoured because the easier handling. In addition the PCB technology has the suitability for applications

in fuel cell stacks, which is a condition precedent for using current density distribution measurements in controlling fuel cell systems. Consequently the PCB technology was improved at the DLR and is used for the investigation of the behavior of fuel cell with various fuel cell designs and flow fields.

#### References

- [1] E. Gülzow, S. Weißhaar, R. Reissner, W. Schröder, J. Power Sources 118 (2003) 405.
- [2] N. Wagner, in: E. Barsoukov, J. Ross Macdonald (Eds.), *Electrochemical Power Sources—Fuel Cells in Impedance Spectroscopy: Theory, Experiment and Applications*, 2nd ed., John Wiley & Sons, Inc., 2005, p. 497.
- [3] S.J.C. Cleghorn, C.R. Derouin, M.S. Wilson, S. Gottesfeld, J. Appl. Electrochem. 28 (1998) 663–672.
- [4] D.J.L. Brett, S. Atkins, N.P. Brandon, V. Vesovic, N. Vasileiadis, A.R. Kucernak, Electrochem. Commun. 3 (11) (2001) 628–632.
- [5] J. Stumper, S.A. Campbell, D.P. Wilkinson, M.C. Johnson, M. Davis, Electrochim. Acta 43 (24) (1998) 3773–3783.
- [6] Z. Liu, Z. Mao, B. Wu, L. Wang, V.M. Schmidt, J. Power Sources 141 (2005) 205–210.
- [7] M. Noponen, T. Mennola, M. Mikkola, T. Hottinen, P. Lund, J. Power Sources 106 (1–2) (2002) 304–312.
- [8] M.M. Mench, C.Y. Wang, J. Electrochem. Soc. 150 (1) (2003) A79–A85.
- [9] A. Hakenjos, H. Muentner, U. Wittstadt, C. Hebling, J. Power Sources 131 (2004) 213–216.
- [10] M.M. Mench, C.Y. Wang, M. Ishikawab, J. Electrochem. Soc. 150 (8) (2003) A1052–A1059.
- [11] N. Rajalakshmi, M. Raja, K.S. Dhathathreyan, J. Power Sources 112 (2002) 331–336.
- [12] K.-H. Hauer, R. Potthast, T. Wüster, D. Stolten, J. Power Sources 143 (2005) 67–74.
- [13] E. Gülzow, T. Kaz, R. Reissner, H. Sander, L. Schilling, M.v. Bradke, J. Power Sources 105 (2002) 261.
- [14] S. Weißhaar, R. Reißner, T. Kaz, E. Gülzow, in: D. Stolten, B. Emonts, R. Peters (Eds.), *Proceedings of the Second European PEFC Forum*, vol. 2, Lucerne, Switzerland, 2003, p. 557.
- [15] P. Metzger, K.A. Friedrich, H. Müller-Steinhagen, G. Schiller, Solid State Ionics 177 (2006) 2045.
- [16] C. Wieser, A. Helmbold, W. Schnurnberger, in: *Int. Symp. on Proton Conducting Fuel Cells*, Electrochem. Soc., vol. 98-272, 1998, p. 457.
- [17] C. Wieser, A. Helmbold, E. Gülzow, J. Appl. Electrochem. 30 (2000) 803.
- [18] Ch. Wieser, Fortschritt-Berichte VDI, Reihe 6, Nr. 454, 2001.
- [19] S. Schönbauer, T. Kaz, H. Sander, E. Gülzow, in: D. Stolten, B. Emonts, R. Peters (Eds.), *Proceedings of the Second European PEFC Forum*, vol. 1, Lucerne, Switzerland, 2003, p. 231.
- [20] S. Schönbauer, T. Kaz, H. Sander, in preparation.
- [21] S. Schönbauer, H. Sander, *Proceedings of the 3rd European PEFC Forum*, July 4–8, 2005, Lucerne, Switzerland, 2005, CD-ROM File No. B056.
- [22] E. Gülzow, S. Schönbauer, FDFC2004, Belfort 29, November 4–2 December, 2004.
- [23] E. Knöri, M. Gülzow, Schulze, *Proceedings of the Third European PEFC Forum*, July 4–8, 2005, Lucerne, Switzerland, 2005, CD-ROM File No. P213.
- [24] S. Weisshaar, R. Reissner, T. Kaz, E. Gülzow, *Proceedings of the Second PEFC Forum*, Lucerne/Switzerland, 30 June–4 July, 2003.
- [25] M. Schulze, E. Gülzow, T. Knöri, *Alteration of cell performance by change of the humidification investigated by electrochemical impedance spectroscopy and current density measurements*, Fuel Cell Seminar 2004, San Antonio, November 2004.